Sputtering yield of indium films bombarded with low energy Ar⁺ ion beams

Authors:
MJ Madito[a]
JJ Terblans[b]
HC Swart[b]
CB Mtshali[a]

Affiliations:
[a]iThemba LABS, National Research Foundation PO Box 722, Somerset West 7129, Cape Town, South Africa
[b]Department of Physics, University of the Free State PO Box 339, Bloemfontein, ZA-9300, South Africa

Corresponding author:
JJ Terblans
E-mail: TerblansJJ@ufs.ac.za

Noble gas ion sputtering combined with Auger electron spectroscopy (AES) analysis has been applied extensively for elemental composition depth profiling of the target materials. Such depth profiles have been used widely not only for elemental composition analysis but also for extracting the sputtering yields of the target materials. Despite a large number of publications on sputtering yields there are only a small number of reports (in literature) on the measured sputtering yields of indium compounds. Indium is used to dope semiconductors for electronic devices (transistor) and thin film solar cells. In order to obtain accurate depth information (for indium thin films) with Ar⁺ ion profiling, it is essential to have reliable sputtering yields for the In metal. In this study, the argon ion sputtering yields of indium films are reported for a range of low ion beam energies (0.5–4.0 keV). The indium films (106 nm) were deposited on SiO_2 substrates under vacuum by electron beam evaporation. The films were subjected to Ar⁺ ion sputtering combined with AES analysis to obtain the depth profiles, which were used to extract the sputtering yield values. The obtained sputtering yield values are in the range of 2 to 6 atoms/ions for Ar⁺ ion beam energies in the range of 0.5–4.0 keV, respectively. The Monte Carlo simulation code, Stopping and Range of Ions in Materials (SRIM) were used to simulate the Ar⁺ ion bombardment of the indium film and to obtain the surface sputtering yields and influences the structures as deposited and the corresponding activities induced. These were also calculated using a semi-empirical formula developed for such predictions. The sputtering yields obtained from SRIM and the semi-empirical formula are in agreement with the experimental values.

Keywords: indium; sputtering yield; depth profiles; argon ions; surface sputtering; SRIM

Verstuiwingsopbrengs van indium vanaf dunlagies gebombardeer met lae energie Ar⁺ ioonbundels: Edelgasioonverstuiwing gekombineer met Auger elektronspekstroskopie (AES) word algemeen gebruik vir die bepaling van die elementsamestelling van die diepteprofiele van die teikenmateriaal. Sulke diepteprofielsamestellings is algemeen gebruik vir element samestellingsanalise asook vir bepaling van die verstuiwingsopbrengs van die teikenmateriaal. Ondanks 'n groot aantal publikasies oor verstuiwingsopbrengs, is daar slegs 'n klein aantal verslae in die literatuur oor die gemete verstuiwingsopbrengs van Indiumverbindings. In word gebruik vir die dotering van halfgeleiers in elektroniese toestelle (transistors) en dunlagies sonselle. Dit is noodsaaklik om betroubare verstuiwingsopbrengs vir die In metaal te hê, vir akkurate diepte inligting (vir In dunlagies) met Ar⁺-ioonprofielering. In hierdie studie word die Ar⁺-ioonverstuiwingsopbrengs vanaf In dunlagies gerapporteer vir 'n reeks lae ioonbundel energieë (0.5 – 4.0 keV). Die In dunlagies (106 nm) is op 'n SiO_2 substraat opgedamp in vakuum deur van elektronbundelopdamping gebruik te maak. Die dunlagies is met Ar⁺-ioonverstuiwing gekombineer met AES analise om die diepteprofielsamestelling te verkry, wat weer gebruik is om die verstuiwingsopbrengs te onttrek. Die verstuiwingsopbrengswaardes is in die orde van 2 tot 6 atome per Ar⁺ ioon vir 'n Ar⁺ ioonbundel met 'n energie tussen 0.5 – 4.0 keV onderskeidelik. Die Monte Carlo simulasie kode, "Stopping and Range of Ions in Materials" (SRIM) is gebruik om die Ar⁺-ioonverstuiwing van die In dunlagie te simuleer en die verstuiwingsopbrengs te verkry. 'n Semi-empiriese formule wat ontwikkel is vir die voorspellings van verstuiwingsopbrengs is ook gebruik om die verstuiwingsopbrengs te bereken. Die verstuiwingsopbrengs verkry vanaf SRIM en die semi-empiriese formule vergelyk goed met die eksperimentele waardes.

Sleutelwoorde: In; Verstuiwingsopbrengs; Diepteprofielsamestelling; Argonioon; Oppervlakteverstuiwing; SRIM

Introduction

In ion beam analysis (IBA), ion beams have been used extensively to investigate damage formation and the evolution of the damage induced by high energy particles in materials. This was done in an attempt to study the effects of exposure to high energy ion bombardment (e.g. see most articles of Nuclear Instruments and Methods in Physics Research Section B: Beam Interactions with Materials and Atoms). On the other hand, the combination of surface spectroscopy techniques [e.g. Auger electron spectroscopy (AES) and X-ray photoelectron spectroscopy (XPS)] and ion gas sputtering (with low ion beam energies) are useful depth profiling analysis techniques to obtain elemental composition with depth (Zalar and Hofmann 1993; Seah 1984). In the semiconductors industry, ion sputtering has become an important fabrication technique.

Sputtering is characterised primarily by the sputtering yield, Y, which is defined as in Eq. 1 (Nastasi et al. 1996)

$$Y = \frac{\text{mean number of emitted atoms}}{\text{incident particle}}. \qquad (1)$$

Experimentally, the Y values are derived from the sputtering rates ($\dot{z}$) (Watts and Wolstenholme 2003; Riviere et al. 2009):

$$\dot{z} = \frac{YI}{e} \qquad (2)$$

where I is the ion beam current and e is the charge on the ion. To know the number of atomic layers removed per second under the beam's rastered area, A, the atomic weight (w) and the density (ρ) of the target material are introduced in equation 2 as follows (Watts and Wolstenholme 2003; Riviere et al. 2009):

$$\dot{z} = \frac{YIw}{eNA\rho} \qquad (3)$$

where N is Avogadro's number.

Moreover, the sputtering yield of the atoms typically depends on ion species, energy and the incident angle, and the target material (structure and composition) (Nastasi et al. 1996). The typical Y values lie in the range of 0.5–10 atoms/ions for the medium mass ion species and keV ion beam energies of general interest in ion-solid interactions (Matsunami et al. 1984; Matsunami et al. 1981; Nastasi et al. 1996).

In view of the collision cascade, the sputtering process involves a series of collisions comprising energy transfer between atoms in the target material, and the most important energy transfer is between the surface atoms of the solid. Therefore, every near-surface interaction or atom collision should be evaluated in detail, and this can be achieved by using the binary collision Monte Carlo simulation code, Stopping and Range of Ions in Materials (SRIM, formerly TRIM) with an option, "Surface Sputtering/Monolayer Collisions". In this option, the sputtered depth (target thickness) of ~3 nm for heavy ions (Z > 5), is adequate. In surface spectroscopy techniques, this depth corresponds to the inelastic mean free path of the Auger electrons (or photoelectrons), which is in the order of a few nm corresponding to the topmost surface atomic layers of the analysed sample (Watts and Wolstenholme 2003; Riviere et al. 2009). It is worth mentioning that although SRIM is preferred, it is not a dynamic code, therefore, in surface sputtering it considers every atomic layer as new without considering the effect of the previous bombardment and this could slightly change the surface sputtering yield (especially under high ion beam energies). Nonetheless, SRIM provides calculations for the trajectories of ions with accurate details of ranges, recoil mixing, transport parameters and so on, and it has been used extensively because of its relative power and ease of use (Ziegler and Biersack 1985; Ziegler et al. 2010). Theoretically, a semi-empirical formula for sputtering of single elemental targets was developed by Matsunami et al. (Matsunami et al. 1984) and Yamamura et al. (Yamamura, et al. 1982) using a combination of Lindhard's theory of nuclear and electronic stopping together with sputtering data. This formula can predict the sputtering yields for any ion-target combination since it accounts for both heavy-ion and light-ion sputtering. Despite a large number of publications on ion beam sputtering, data on the sputtering yield of indium is lacking in literature. Herein, we report on the AES-argon ion sputtering yield of an indium film deposited on a SiO_2 substrate by electron beam evaporation, which ultimately significantly influences the activities of the material as direct function of the structures as deposited. The obtained experimental sputtering yield values are compared to SRIM and semi-empirical formula sputtering yields.

Experimental

The SiO_2 substrates used in this study were prepared by wet oxidation of Si(100) at 1000 °C for 1 h in a Lindberg tube furnace. Indium films (106 nm) were evaporated onto SiO_2 substrates by electron beam evaporation. Before indium evaporation, pure Ti was evaporated to clean the residual oxygen in the chamber to avoid indium oxidisation. During the evaporation, the base pressure in the vacuum chamber was 2.5×10^{-5} Torr. The film's thicknesses were monitored during the evaporation with a calibrated Inficon Leybold Heraeus XTC thin film monitor.

The indium films were subjected to Ar^+ ion sputtering combined with Auger electron spectroscopy analysis (AES) to obtain the depth profiles. Auger peak to peak heights (APPHs) were recorded as a function of the sputtering time for In (301-440 eV), O (450-530 eV), Si (60-105 eV) and C (230-300 eV) and were converted to fractional concentration using Palmberg equation and the correction factors as discussed by Seah and Gilmore (Seah and Gilmore 1998). The correction factors include the backscattering factor, inelastic mean free path (IMFP) of Auger electrons

(calculated with the TPP-2M formula (Tanuma et al. 2005), the atomic density and elastic scattering factor. The sensitivity factors used were determined from pure elemental standards under the same conditions used for the depth profiles. The Auger measurements were carried out in a PHI 600 Scanning Auger system using a cylindrical mirror analyser (CMA) with a co-axial electron gun. During analysis, the base pressure in the main chamber was 9.0×10^{-8} Torr and the ion gun was operated at an argon pressure of 3.4×10^{-5} Torr in the ionisation chamber. The ion gun was operated at a beam voltage in the range of 0.5–4.0 keV and the beam was rastered over a 2×2 mm^2 area. A 10 keV primary electron beam with a diameter of ~10 μm and current of 4.8 μA was used for the AES measurements. The sample was tilted with the normal of the film surface at 30° with respect to the direction of the incident *electron* beam and 50° with respect to the direction of the incident *ion* beam. A Faraday cup with a hole (diameter = 300 μm) was used to obtain the ion beam current density, and the current was measured with a Keithley's picoammeter (model 6485). The ion beam stability was monitored by measuring the ion beam current before and immediately after depth profiling.

Results and discussion

Figure 1(a) to 1(e) show the AES depth profiles obtained from 106 nm thick indium films sputtered with Ar$^+$ ion beam energies in the range of 0.5–4.0 keV, respectively. These elemental composition depth profiles show the indium layer followed by a SiO$_2$ substrate. The Auger spectrum of the sputter cleaned surface of the indium film (Figure 1(f)) confirms the high purity of the film (i.e. within the detection limit of the Auger spectroscopy). In addition, the spectrum shows prominent peaks at 405 and 412 eV which corresponds to the MNN Auger transitions of indium. The C and O peaks observed from the Auger spectrum of the as-received sample are due to adsorbed species from sample handling in air. From the depth profiles, it can be seen that the sputtering time required to completely etch a film, reduces with increasing ion beam energy. This means that the sputtering rate ($\dot{z}$) increases with the ion beam current (Eq. 2) which correspondingly increases with increasing ion beam energy, as shown by Figure 2(a). Furthermore, from the $\dot{z}$ values, the sputtering yield was obtained using equation 3 (see Figure 2(b)). The error in these values is primarily due to ion beam current density measurements/stability, which was monitored.

SRIM was further used to simulate the Ar$^+$ ion sputtering of the indium film with low ion beam energies in the range of 0.5–4.0 keV at normal incidence, as shown in Figure 3. The simulation was carried out using the SRIM -2013 version, and "Surface Sputtering/Monolayer Collisions" option. The software default values of threshold displacement and lattice binding energies were used. 10 000 incident ions were used to improve the statistics. Figure 3(a) shows the increase in the ion's projected range, R_p and the total target atom's displacements with increasing ion beam energy,

suggesting a linear cascade regime which is applicable for medium mass ions such as Ar$^+$. In the linear cascade regime, the total number of recoils is proportional to the energy deposited per unit depth in nuclear energy loss (Nastasi et al. 1996). In SRIM the incident ions and the recoil atoms in the target material are followed throughout their de-acceleration until their energy falls below the determined energy, i.e. cut-off energy of 5 eV for incident ions, and 2.49 eV (surface binding energy) for indium recoiling atoms, in this case. In Figure 3(a), the sputtered depth is within 3 nm corresponding to the topmost surface atomic layers of the target. Furthermore, as Ar$^+$ ions come to rest in the indium film, they lose energy via electronic and nuclear collision processes (Figure 3(b)). The latter process is responsible for atom's recoil and some of these recoils (backward recoils) have enough energy to escape from the solid make-up and sputtering yield (Figure 3(c)). The electron energy loss further induces point defects (vacancy-interstitial defects), with the experimental sputtering yield values in agreement with the values from SRIM, which confirms that the yield is constituted by the nuclear energy-loss mechanism (linear cascade regime), as expected for Ar$^+$ ions.

Moreover, the sputtering yield of the indium film was further calculated using the semi-empirical formula developed by Matsunami et al. (Matsunami et al. 1984; Matsunami et al. 1981) and Yamamura et al. (Yamamura et al. 1982), which is given by Eq. 4.

$$Y_E(E) = 0.42 \frac{\alpha_S Q_S S_n(E)}{U_0 \left[1 + 0.35 U_0 S_e(\varepsilon)\right]} \left[1 - \left(E_{th}/E\right)^{0.5}\right]^{2.8} \tag{4}$$

This holds for ions with energy, E, at normal incidence, where α_S and Q_S are empirical parameters extracted from experimental sputtering data, E_{th} is the sputtering threshold energy, $S_e(\varepsilon)$ is the reduced Lindhard electronic stopping cross-section, $S_n(E)$ is the nuclear stopping cross-section, and U_0 is the surface binding energy.

The parameters in Eq. 4 are defined by Eqs. 5 to 11 below, and are as follows (Nastasi et al. 1996; Matsunami et al.; 1984, Matsunami et al. 1981; Yamamura, et al. 1982) :

$$E_{th} = \left(\frac{2M_1 + 2M_2}{M_1 + 2M_2}\right)^6 \frac{U_0}{\gamma}, \quad \text{vir} \quad M_1 < M_2 \tag{5}$$

where M_1 and M_2 are the masses of the incident ion and the target atom, respectively, γ is the energy-transfer factor for elastic collisions given by

$$\gamma = \frac{4M_1 M_2}{\left(M_1 + M_2\right)^2}. \tag{6}$$

The nuclear stopping cross-section is given by

$$S_n(E) = K_n S_n(\varepsilon) \tag{7}$$

where

$$K_n = \frac{8.478 Z_1 Z_2}{\left(Z_1^{2/3} + Z_2^{2/3}\right)^{1/2}} \frac{M_1}{\left(M_1 + M_2\right)} \tag{8}$$
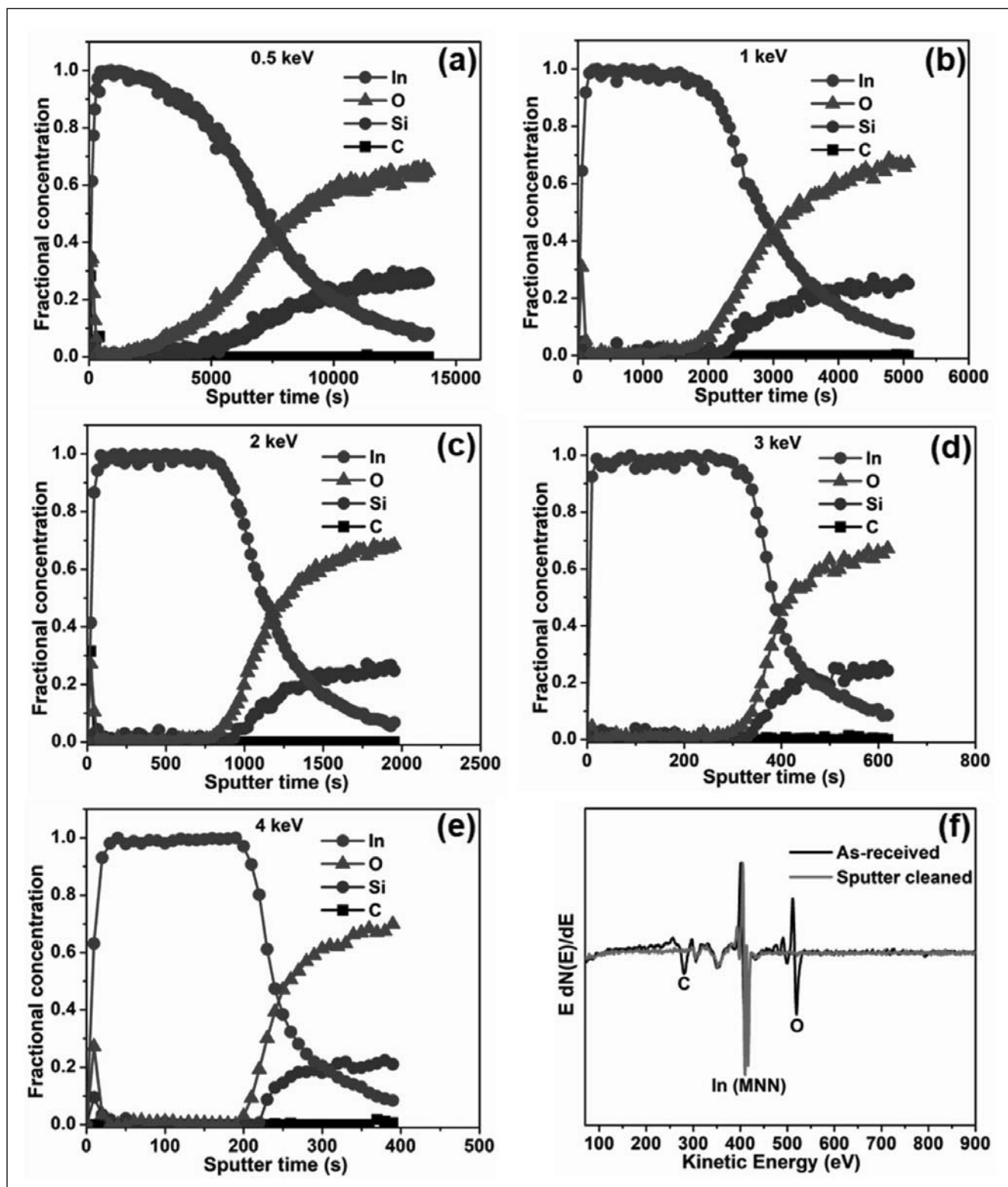
FIGURE 1: (a)-(e) AES depth profiles obtained from the 106 nm thick indium film sputtered with varying Ar⁺ ion beam energies in the range of 0.5–4.0 keV. (f) Auger spectra of as-received and the sputter cleaned surface of the indium film.
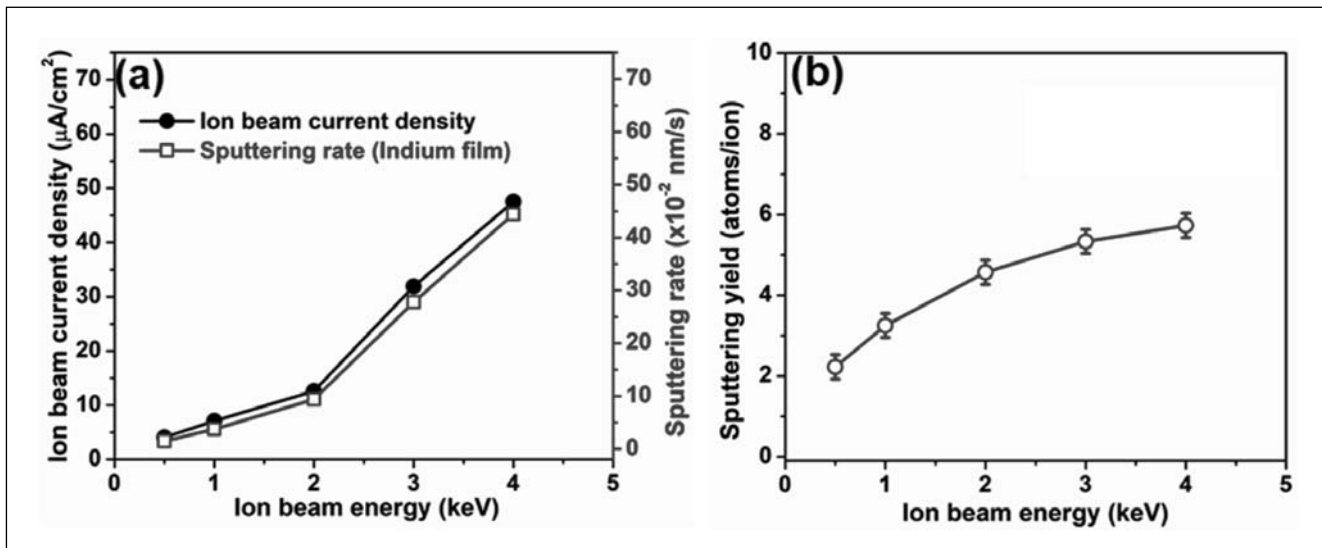
FIGURE 2: (a) Ion beam current density and the sputtering rate of the indium film as a function of ion beam energy and (b) the corresponding sputtering yield.
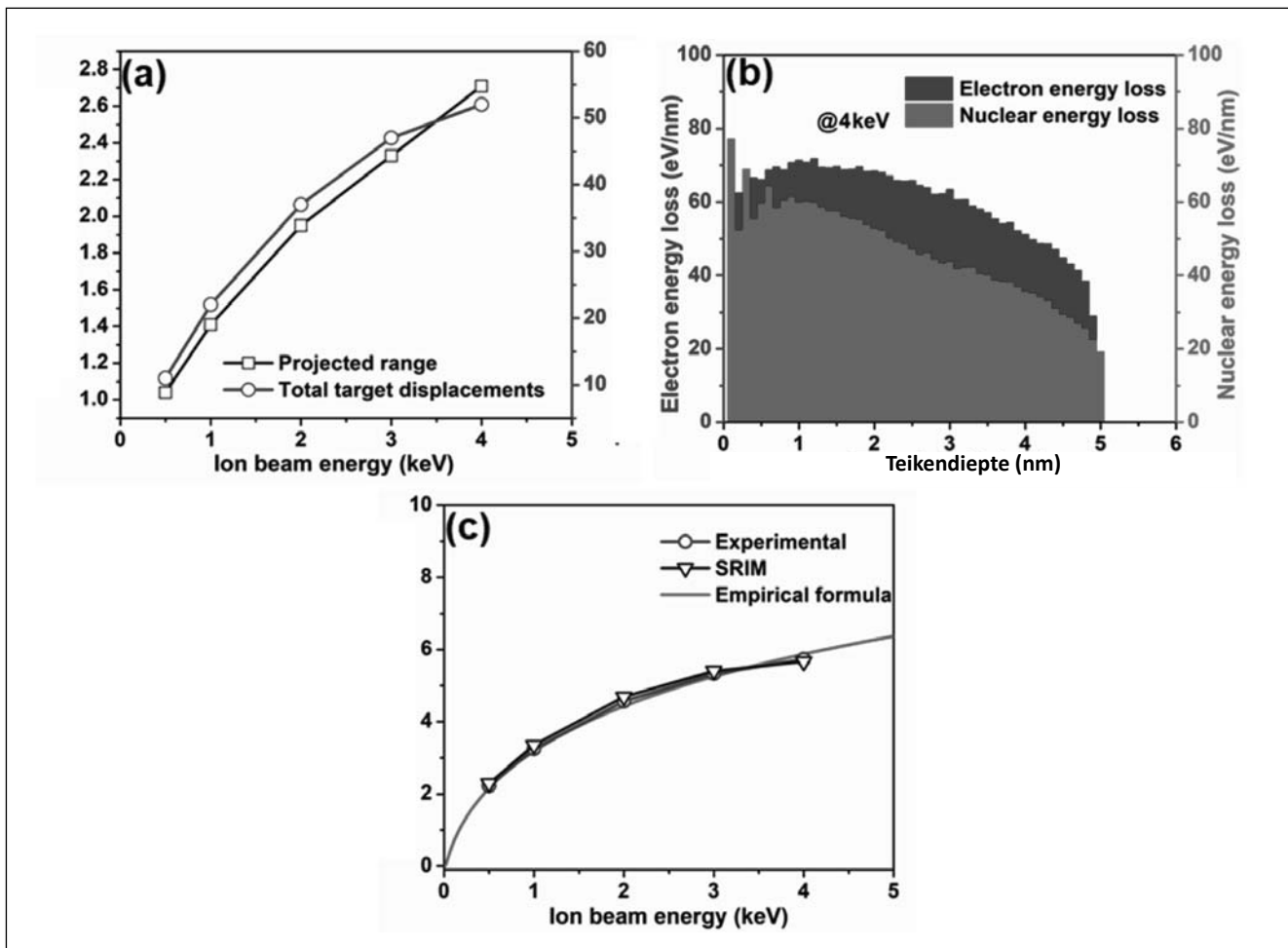

FIGURE 3: (a) The ion projected range, R_p and the total target atom's displacements as a function of ion beam energy. (b) The electron and nuclear energy loss with depth for incident 4 keV Ar+ ion beam energy. (c) Comparison of SRIM, experimental and semi-empirical formula sputtering yield as a function of incident Ar+ ion beam energy.

and

$$S_n(\varepsilon) = \frac{3.441\varepsilon^{1/2}\ln(\varepsilon + 2.718)}{1 + 6.355\varepsilon^{1/2} + \varepsilon(6.882\varepsilon^{1/2} - 1.708)}. \quad (9)$$

In equation 8, Z_1 and Z_2 are the element atomic numbers of the incident ion and the target material, respectively, and the energy, ε (eV), in equation 9 is given by

$$\varepsilon = \frac{0.03255}{Z_1 Z_2 (Z_1^{2/3} + Z_2^{2/3})^{1/2}} \frac{M_1}{(M_1 + M_2)} E \quad (10)$$

Although α_S and Q_S are extracted from fitting the experimental sputtering data with equation 4, the empirical expression for α_S is given by

$$\alpha_S = 0.10 + 0.155(M_2/M_1)^{0.73} + 0.001(M_2/M_1)^{1.5} \quad (11)$$

The values of the parameters (Eqs. 5 to 11) used in Eq. 4 to obtain the sputtering yield of indium are listed in Table I. The sputtering yield of indium as calculated using the semi-empirical formula (Eq. 4) and the parameters are also

listed in Table I. The results are shown in Table II and Figure 3(c). It is clear that the measured sputtering yields were in good agreement with the sputtering yields calculated with the semi-empirical formula and SRIM calculations. These results are summarised in Table II.

TABLE I: The parameters used to calculate the sputtering yield of indium.

Parameter	Waarde
E (eV)	0 – 10000
M_1/M_2	39.96/114.82
Z_1/Z_2	18/49
γ	0.766
Q_S	1.06
U_0 (eV)	2.49
E_{th} (eV)	7.45
α_S	0.440
ε (eV)	0 - 0.021 for E = 0 - 10000 eV
K_n (10^{-15} eV cm^2)	428.9
S_n (ε)	0 - 0.264 for E = 0-10000 eV
S_e (ε)	0 - 0.041 for E = 0-10000 eV

TABLE II: The experimental data (ion beam energy and current density and the corresponding sputtering rate and yield values), SRIM and semi-empirical formula sputtering yields for indium.

Ion beam energy (keV)	Ion beam current density (µA/cm²)	Sputtering rate (×10⁻² nm/s)	Experimental (Y) (atoms/ions) ±0.3	SRIM (Y) (atoms/ions)	Semi-empirical formula (Y) (atoms/ions)
0.5	4.1	1.49	2.2	2.29	2.16
1.0	7.1	3.77	3.2	3.35	3.18
2.0	12.6	9.40	4.6	4.69	4.43
3.0	31.9	27.78	5.3	5.41	5.25
4.0	47.5	44.44	5.7	5.67	5.87

Conclusion

In this study, the indium films were deposited on SiO_2 substrates under vacuum by electron beam evaporation, and thereafter, were subjected to Ar^+ ion sputtering (with ion beam energies in the range of 0.5–4.0 keV) combined with AES analysis to obtain the depth profiles, which were used to extract the sputtering yield values. The sputtering yields of indium were also calculated using SRIM and the empirical formula developed by Matsunami et al. (Matsunami et al. 1984; Matsunami et al. 1981) and Yamamura et al. (Yamamura et al. 1982). The sputtering yields obtained from SRIM and semi-empirical calculations were found to be in good agreement with the experimental values.

Acknowledgments

References

Matsunami N, Yamamura Y, Itikawa Y, Itoh N, Kazumata Y, Miyagawa S, Morita K, Shimizu R. 1981. A semiempirical formula for the energy dependence of the sputtering yield, *Radiation Effects*, 57, 15–21.

Matsunami N, Yamamura Y, Itikawa Y, Itoh N, Kazumata Y, Miyagawa S, Morita K, Shimizu R, Tawara H. 1984. Energy dependence of the ion-induced sputtering yields of monatomic solids, *Atomic Data and Nuclear Data Tables*, 31, 1–80.

Nastasi M, Mayer JW, Hirvonen JK. 1996. *Cambridge Solid State Science Series: Ion-Solid Interactions: Fundamentals and Applications*, Cambridge University Press, Cambridge.

Riviere JC, Myhra S, Myhra S. 2009. *Handbook of Surface and Interface Analysis*, CRC Press.

Seah MP. 1984. A review of the analysis of surfaces and thin films by AES and XPS, *Vacuum*, 34, 463–478.

Seah MP, Gilmore IS. 1998. Quantitative AES. VIII: analysis of auger electron intensities from elemental data in a digital auger database, *Surface and Interface Analysis*. 26, 908–929.

Tanuma S, Powell CJ, Penn DR. 2005. Calculations of electron inelastic mean free paths, *Surface and Interface Analysis*. 37, 1–14.

Watts JF, Wolstenholme J. 2003. *An introduction to surface analysis by XPS and AES*, John Wiley & Sons, Inc., New York.

Yamamura Y, Matsunami N, Itoh, N. 1982. A new empirical formula for the sputtering yield, *Radiation Effects*, 68, 83–87.

Zalar A, Hofmann S. 1993. Comparison of rotational depth profiling with AES and XPS, *Applied Surface Science*, 68, 361–367.

Ziegler JF, Biersack JP. 1985. *Treatise on Heavy-Ion Science: The Stopping and Range of Ions in Matter*, Springer US, Boston, MA, pp. 93–129.

Ziegler JF, Ziegler MD. Biersack, J.P. 2010. SRIM – The stopping and range of ions in matter (2010), *Nuclear Instruments and Methods in Physics Research Section B: Beam Interactions with Materials and Atoms,* 268, 1818–1823.